



**HAL**  
open science

## Energy-based design of dynamic allocation in the presence of saturating actuators

Thiago A Lima, Sophie Tarbouriech, Bismark C Torrico, Fabrício G Nogueira

► **To cite this version:**

Thiago A Lima, Sophie Tarbouriech, Bismark C Torrico, Fabrício G Nogueira. Energy-based design of dynamic allocation in the presence of saturating actuators. 24th International Symposium on Mathematical Theory of Networks and Systems MTNS 2020, Aug 2021, Cambridge, United Kingdom. 10.1016/j.ifacol.2021.06.087 . hal-03192785

**HAL Id: hal-03192785**

**<https://hal.science/hal-03192785v1>**

Submitted on 9 Apr 2021

**HAL** is a multi-disciplinary open access archive for the deposit and dissemination of scientific research documents, whether they are published or not. The documents may come from teaching and research institutions in France or abroad, or from public or private research centers.

L'archive ouverte pluridisciplinaire **HAL**, est destinée au dépôt et à la diffusion de documents scientifiques de niveau recherche, publiés ou non, émanant des établissements d'enseignement et de recherche français ou étrangers, des laboratoires publics ou privés.

# Energy-based design of dynamic allocation in the presence of saturating actuators\*

Thiago A. Lima\*   Sophie Tarbouriech   Bismark C. Torrico   Fabrício G. Nogueira

April 8, 2021

## Abstract

This paper addresses the design of dynamic allocation functions for systems with saturating actuators. The novelty of the proposal relies on the use of an anti-windup loop to drive the state of the allocator, which in some sense dynamically compensates the difference between the computed control signal and the plant input. Furthermore, the co-design of the allocator and anti-windup loop is presented, allowing to deal with the multiple objective of reducing the allocator error and increasing the closed-loop region of stability. Theoretical conditions are derived in terms of linear matrix inequalities (LMIs) and an optimization scheme consisting in the minimization of the energy of the allocator error is proposed. Two examples borrowed from the literature illustrate the proposed technique and show its effectiveness.

## 1 Introduction

Control allocation is widely used in over-actuated systems where the controlled plant is, in general, modeled using torques and forces as inputs, and these forces and torques are generated by the set of actuators (for example microthrusters in space applications) that together produce the desired control effort. As pointed out in [13], the advantages with the use of the control allocation approach is, in general, modularity and ability to handle constraints.

The control allocation problem is treated in several papers dealing with specific applications, in particular in the aeronautical or spatial contexts: see, for example, the works of [5], [8], [1], [3]. Technical solutions are also proposed in the literature from a theoretical point of view. Both the works in [4] and [10] consider the output regulation problem of over-actuated systems in the presence of full-information regarding the system states and exogenous inputs. More specifically, [4] proposes allocation mechanism that takes the form of a hybrid system and accounts for input constraints. In [9], optimization-based algorithms, as interior point method, are detailed in order to compute the optimal static allocation.

[6] note that control allocation functions have the primary objective of ensuring that the controller output (noted  $y_c$  in the paper) is produced jointly by the multiple effectors. Thus, given the influence matrix (noted  $M$  in the paper), we want to make sure that the input signal (noted  $u_p$  in the paper) is equal to the computed control signal ( $y_c$ ) or that at least the error between them is very small.

The objective pursued in the current paper can be viewed as in the same vein. Indeed, the paper proposes the co-design of a dynamic allocation function and anti-windup loop with the focus of minimizing the allocation error and maximizing the estimation of the region of stability of the closed loop. Although dynamic allocation function has been proposed in [14], there are some fundamental differences with the strategy in

---

\*Manuscript accepted for publication at the 24th International Symposium on Mathematical Theory of Networks and Systems (MTNS 2020). This study was financed in part by the Coordenação de Aperfeiçoamento de Pessoal de Nível Superior - Brasil (Capes) - Finance Code 001, and by ANR project HANDY 18-CE40-0010.

Sophie Tarbouriech is with LAAS-CNRS, Université de Toulouse, CNRS, Toulouse, France (e-mail: tarbour@laas.fr).

Thiago A. Lima\*, Fabrício G. Nogueira and Bismark C. Torrico are also with the Department of Electrical Engineering, Federal University of Ceará, Fortaleza, Brazil (e-mail:thiago.lima@alu.ufc.br, fnogueira@dee.ufc.br, bismark@dee.ufc.br).

this paper that can be shortly listed: i) [14] does not consider the co-design problem of the anti-windup loop and allocation. ii) The parameters of the allocator in [14] are manually selected. iii) The formulation in [14] is focused in the specific case where the size of the plant input (noted  $m_c$  in the paper) is equal to the size of allocator output (noted  $m_a$  in the paper) and the influence matrix is the identity matrix (i.e.,  $M = I$ ). In the current work, we can deal with broader range of systems since we consider the case of  $m_a \geq m_c$ .

By considering a Lyapunov-based approach, theoretical conditions are derived in terms of linear matrix inequalities (LMIs) in order to solve the co-design of the allocator and anti-windup loop. Furthermore, an optimization scheme consisting in the minimization of the energy of the allocator error is proposed. Its use in two examples borrowed from the literature shows its effectiveness.

The paper is organized as follows. Section 2 is dedicated to present the general view of the control allocation, and to specify the class of the plant, controller and allocation function under consideration. Section 3 presents the main theoretical conditions, together with the associated optimization scheme. In Section 4, two examples borrowed from the literature emphasize the interest of the proposed approach. Finally, in Section 5, concluding remarks and forthcoming issues end the paper.

**Notation.** For a matrix  $Y \in \mathbb{R}^{n \times m}$ ,  $Y^\top \in \mathbb{R}^{m \times n}$  means its transpose,  $Y_{(i)}$  denotes its  $i$ th row, while for  $v \in \mathbb{R}^m$ ,  $v_{(i)}$  denotes its  $i$ th component. For matrices  $W = W^\top \in \mathbb{R}^{n \times n}$  and  $Z = Z^\top \in \mathbb{R}^{n \times n}$ ,  $W > Z$  means that  $W - Z$  is positive definite. Likewise,  $W \geq Z$  means that  $W - Z$  is positive semi-definite.  $I$  and  $0$  denote identity and null matrices of appropriate dimensions, although their dimensions can be explicitly presented whenever relevant. In this case,  $0_{n \times m}$  represents the  $n \times m$  null matrix, while  $I_n$  represents  $n \times n$  identity matrix. The  $\star$  in  $\begin{bmatrix} A & B \\ \star & C \end{bmatrix}$  denotes symmetric blocks in the expression of a matrix, that is  $\star = B^\top$ . Finally, for matrices  $W$  and  $Z$ ,  $\text{diag}(W, Z) = \begin{bmatrix} W & 0 \\ 0 & Z \end{bmatrix}$  where the null matrices  $0$  are of appropriate dimensions.

## 2 Problem formulation

### 2.1 General view

Consider the general view of the control allocation problem shown in Fig. 1.

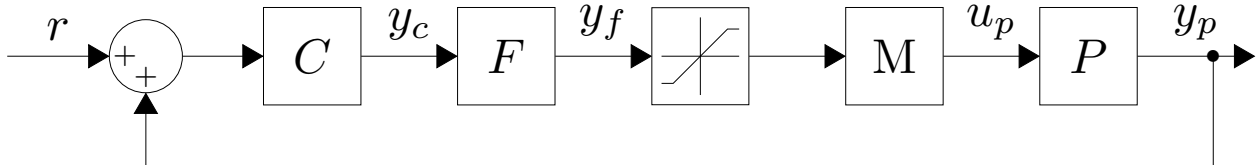


Figure 1: General view of control allocation problem.

Subsystems  $C$ ,  $F$ ,  $M$ , and  $P$  are the controller, the control allocator, the influence matrix and the plant, respectively. The plant is driven by  $u_p \in \mathbb{R}^{m_c}$  inputs. The controller computes a set of desired  $y_c \in \mathbb{R}^{m_c}$  efforts that must be injected in the plant in ideal conditions. The plant input is generated by a set of  $m_a \geq m_c$  actuators, represented by the signal  $y_f \in \mathbb{R}^{m_a}$ . In the absence of nonlinearities,  $u_p = My_f$ , and the so-called influence matrix  $M \in \mathbb{R}^{m_a \times m_c}$  maps how each individual effort of the  $m_a$  actuators combines to generate the inputs acting on the plant. The simplest allocation function is given by the right pseudo-inverse of  $M$ , that is,  $F = M^\dagger$ , with  $MM^\dagger = I$ .

In case the actuators are subject to amplitude limits, the process input,  $u_p$ , is given by  $u_p = Msat(y_f)$ , where the standard decentralized saturation function is defined as

$$sat(y_{f(i)}) = sign(y_{f(i)}) \min\{|y_{f(i)}|, \bar{u}_{(i)}\}, \bar{u}_{(i)} > 0, \quad (1)$$

for  $i = 1, \dots, m_a$ , where  $\bar{u}_{(i)}$  denotes the amplitude bound in each actuator.

In this case, two main problems arise: i) Guarantees of stability of the closed-loop in the presence of saturation need to be ensured. ii) The application of the pseudo-inverse of  $M$  no longer produces null error between the plant input and the controller output. In this context, more complex allocation functions with the ability to handle redundancy and constraints should be applied.

## 2.2 Plant and controller description

Consider the plant  $P$  described by the following equations

$$P \sim \begin{cases} \dot{x}_p = A_p x_p + B_p u_p, \\ y_p = C_p x_p, \end{cases} \quad (2)$$

where  $x_p \in \mathbb{R}^{n_p}$  is the plant state vector,  $u_p \in \mathbb{R}^{m_c}$  is the plant input,  $y_p \in \mathbb{R}^q$  is the measured output.  $A_p$ ,  $B_p$ , and  $C_p$  are all constant and known matrices of appropriate dimensions. Furthermore, the pairs  $(A_p, B_p)$  and  $(C_p, A_p)$  are supposed to be controllable and observable.

Let us assume that the plant (2) is stabilized by a dynamic output controller  $C$  linearly designed via the connection  $u_p = y_c$ , that is without taking into account the saturation. The controller  $C$  is defined by the following equations

$$C \sim \begin{cases} \dot{x}_c = A_c x_c + B_c y_p + v_{aw}, \\ y_c = C_c x_c + D_c y_p, \end{cases} \quad (3)$$

where  $x_c \in \mathbb{R}^{n_c}$  is the controller state vector and  $y_c \in \mathbb{R}^{m_c}$  is the controller output.  $A_c$ ,  $B_c$ ,  $C_c$ , and  $D_c$  are supposed known. The anti-windup compensation signal  $v_{aw}$  is added in order to mitigate the undesired effects of saturation (see, for example, [12], [15]). In this paper, we consider the anti-windup signal  $v_{aw} = E_c \varphi(y_f)$ ,  $E_c \in \mathbb{R}^{n_c \times m_a}$ , with the deadzone  $\varphi(y_f)$  defined as

$$\varphi(y_f) = \text{sat}(y_f) - y_f \quad (4)$$

where the saturation map is defined from (1) and  $y_f$  is the output of the allocation function.

**Remark 1.** *By construction, the linear connection plant-controller is supposed to be stable. In other words, the controller (3) (with  $v_{aw} = 0$ ) stabilizes the plant (2) through the linear interconnection  $u_p = y_c$  and therefore the following matrix is Hurwitz*

$$A_0 = \begin{bmatrix} A_p + B_p D_c C_p & B_p C_c \\ B_c C_p & A_c \end{bmatrix} \quad (5)$$

## 2.3 Dynamic allocation function description

Consider the influence matrix  $M \in \mathbb{R}^{m_c \times m_a}$ , with  $m_a \geq m_c$ . Let  $\eta = \{\eta_1, \eta_2, \dots, \eta_{n_f}\}$ , with  $n_f = m_a - \text{rank}(M)$ , be a basis for the Kernel of  $M$ . We then propose the following dynamic allocation function

$$F \sim \begin{cases} \dot{x}_f = A_f x_f + E_f \varphi(y_f), \\ y_f = N x_f + M^\dagger y_c, \end{cases} \quad (6)$$

where  $N = [\eta_1 \ \eta_2 \ \dots \ \eta_{n_f}] \in \mathbb{R}^{m_a \times n_f}$ ,  $M^\dagger \in \mathbb{R}^{m_a \times m_c}$  is such that  $MM^\dagger = I$ ,  $x_f \in \mathbb{R}^{n_f}$  is the allocator state vector, and  $y_f \in \mathbb{R}^{m_a}$  is the allocator output. Matrices  $A_f$  and  $E_f$  must be designed to achieve desired behavior of the allocator by taking into account the presence of saturation.

**Remark 2.** *This allocation format is particularly interesting since it has potential to couple with the main requirement of allocation functions, which is to reduce the error between the required plant input signal computed by the controller and the plant actual input. When the system is not saturated,  $u_p = M y_f = y_c$*

since  $MM^\dagger = I$  and  $MN = 0$ . During saturation occurrence,  $u_p = \text{Msat}(Nx_f + M^\dagger y_c)$  and the state  $x_f$  is used to improve system behavior and somehow redistribute the control effort between the actuators. The term  $E_f \varphi(y_f)$  plays an important role since it uses the difference between the saturated actuator output and the required signal.

Let us define the allocator error as  $e = u_p - y_c$ , then  $e = \text{Msat}(y_f) - y_c$ . Using identity (4), the expression  $e = M(Nx_f + \varphi(y_f))$  is easily obtained. Thus, the mapping  $y_c \rightarrow e$  can be defined

$$y_c \rightarrow e \triangleq \begin{cases} \dot{x}_f = A_f x_f + E_f \varphi(y_f), \\ y_f = Nx_f + M^\dagger y_c, \\ e = M(Nx_f + \varphi(y_f)) \end{cases} \quad (7)$$

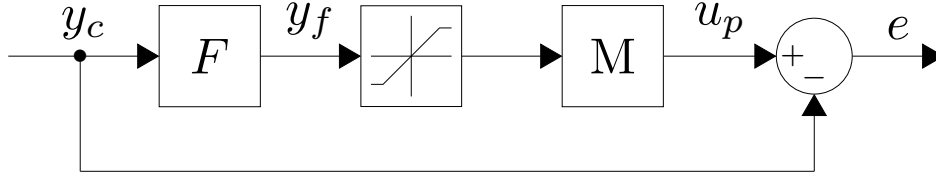


Figure 2: Diagram illustrating mapping from  $y_c$  to allocator error  $e$ .

Note that due to  $MN = 0$ , in the absence of saturation one gets  $e = 0$ .

**Remark 3.** In the rest of the paper, we kept the product  $MN$  in the expression of  $e$  in order to preserve the general format of the allocator and then to be able to deal with the case studied in [14]. See also Section 3.2.

## 2.4 Closed-loop system and problem formulation

By taking into account the definitions of  $P$ ,  $C$  and  $F$ , identity (4) and the connection  $u_p = \text{Msat}(y_f)$ , the complete closed-loop system with  $x = [x_p^\top \quad x_c^\top \quad x_f^\top]^\top \in \mathbb{R}^n$ ,  $n = n_p + n_c + n_f$ , can be written as

$$\begin{cases} \dot{x} = Ax + B_\varphi \varphi(y_f) \\ y_f = Cx \\ e = Hx + M\varphi(y_f), \end{cases} \quad (8)$$

where  $A = \bar{A} + L_f A_f L_f^\top$ ,  $B_\varphi = B_1 + LE$ , with

$$\bar{A} = \begin{bmatrix} A_p + B_p D_c C_p & B_p C_c & 0 \\ B_c C_p & A_c & 0 \\ 0 & 0 & 0 \end{bmatrix}, B_1 = \begin{bmatrix} B_p M \\ 0_{n_c \times m_a} \\ 0_{n_f \times m_a} \end{bmatrix}, E = \begin{bmatrix} E_c \\ E_f \end{bmatrix}$$

$$L = \begin{bmatrix} 0_{n_p \times n_c} & \overbrace{0_{n_p \times n_f}}^{L_f} \\ I_{n_c} & 0_{n_c \times n_f} \\ 0_{n_f \times n_c} & I_{n_f} \end{bmatrix}, \begin{bmatrix} C \\ H \end{bmatrix} = \begin{bmatrix} M^\dagger D_c C_p & M^\dagger C_c & N \\ 0 & 0 & MN \end{bmatrix}.$$

The presence of the dead-zone in the closed-loop dynamics (8) implies to characterize a suitable region of the state space in which the stability is ensured (see, for example, [12], [15]). In general the global asymptotic stability of the origin (that is for any initial condition  $x(0) \in \mathbb{R}^n$ ) does not hold except if the open loop has suitable properties of stability [11]. Hence, the regional stability (that is, only for initial conditions in a neighborhood of the origin) has to be studied. Since exact characterization of the basin of attraction of

the origin remains an open problem, a challenging problem consists in providing an estimate of the basin of attraction as accurate as possible.

Furthermore, we want to ensure some level of performance to the allocator in terms of the error  $e$ , which can be done by imposing conditions that limit the energy of this signal. With respect to (3) and (6), the main objective of this paper is to propose the co-design of the dynamic allocation function, that is  $A_f$ , and  $E_f$ , along with the controller anti-windup gain  $E_c$ . Then the problem we intend to solve can be summarized as follows.

**Problem 1.** *Design matrices  $A_f$ ,  $E_f$  and  $E_c$ , such that*

1. *the regional asymptotically stability of the closed-loop system (8) is ensured and the estimate of the region of attraction is maximized.*
2. *the energy of the allocator error is minimized.*

## 3 Main results

### 3.1 Theoretical conditions

For vectors  $y_f \in \mathbb{R}^{m_a}$  and  $\theta \in \mathbb{R}^{m_a}$ , consider the set

$$\mathbb{S} = \{y_f; \theta; -\bar{u}_{(i)} \leq y_{f(i)} - \theta_{(i)} \leq \bar{u}_{(i)}, i = 1, \dots, m_a\}, \quad (9)$$

and recall the following Lemma from p.43 in [12].

**Lemma 1.** *If  $y_f$  and  $\theta$  belong to set  $\mathbb{S}$ , then the deadzone nonlinearity  $\varphi(y_f)$  satisfies the following inequality, which is true for any diagonal positive definite matrix  $T \in \mathbb{R}^{m_a \times m_a}$*

$$\varphi^\top(y_f)T[\varphi(y_f) + \theta] \leq 0. \quad (10)$$

The following theorem provides a solution to Problem 1.

**Theorem 1.** *Assume there exist positive definite matrices  $\bar{P} = \bar{P}^\top \in \mathbb{R}^{n \times n}$ ,  $\bar{R} = \bar{R}^\top \in \mathbb{R}^{m_c \times m_c}$ , positive definite diagonal matrix  $S = S^\top \in \mathbb{R}^{m_a \times m_a}$ , matrices  $\bar{G} \in \mathbb{R}^{m_a \times n}$ ,  $X_{11} \in \mathbb{R}^{n_p \times n_p}$ ,  $X_{12} \in \mathbb{R}^{n_p \times n_c}$ ,  $X_{21} \in \mathbb{R}^{n_c \times n_p}$ ,  $X_{22} \in \mathbb{R}^{n_c \times n_c}$ ,  $X_{31} \in \mathbb{R}^{n_f \times n_p}$ ,  $X_{32} \in \mathbb{R}^{n_f \times n_c}$ ,  $X_{33} \in \mathbb{R}^{n_f \times n_f}$ ,  $K_f \in \mathbb{R}^{n_f \times n_f}$ ,  $K_e \in \mathbb{R}^{(n_c+n_f) \times m_a}$  such that*

$$\bar{\Psi} = \begin{bmatrix} -\bar{X} - \bar{X}^\top & \bar{\Psi}_{12} & \bar{\Psi}_{13} & 0 \\ \star & \bar{\Psi}_{22} & \bar{\Psi}_{23} & -\bar{X}H^\top \\ \star & \star & -2S & -SM^\top \\ \star & \star & \star & -\bar{R} \end{bmatrix} < 0, \quad (11)$$

$$\begin{bmatrix} \bar{P} & \bar{G}^\top \\ \star & \bar{u}_{(i)}^2 \end{bmatrix} \geq 0, \quad (12)$$

hold with  $\bar{\Psi}_{12} = \bar{P} + J + \bar{A}\bar{X}^\top - \bar{X}$ ,  $\bar{\Psi}_{13} = B_1S + LK_e$ ,  $\bar{\Psi}_{22} = J + J^\top + \bar{A}\bar{X}^\top + \bar{X}\bar{A}^\top$ ,  $\bar{\Psi}_{23} = \bar{\Psi}_{13} + \bar{G}^\top - \bar{X}C^\top$ ,

$$\bar{X} = \begin{bmatrix} X_{11} & X_{12} & 0 \\ X_{21} & X_{22} & 0 \\ X_{31} & X_{32} & X_{33} \end{bmatrix}, \quad J = \begin{bmatrix} 0 & 0 & 0 \\ 0 & 0 & 0 \\ 0 & 0 & K_f \end{bmatrix}.$$

Then, matrices  $E = [E_c^\top \quad E_f^\top]^\top = K_e S^{-1}$ ,  $A_f = K_f X_{33}^{-1\top}$  are solution to Problem 1. In other words:

1. *the closed-loop system (8) is asymptotically stable in the ellipsoid  $\varepsilon(P, 1) = \{x \in \mathbb{R}^n; x^\top P x \leq 1\}$ , with  $P = \bar{X}\bar{P}\bar{X}^\top$  and  $X = \bar{X}^{-1}$ ;*

2. the energy of the error signal is limited and given by  $\int_0^\infty e(\tau)^\top \text{Re}(\tau) d\tau < 1$ , with  $\text{R} = \bar{\text{R}}^{-1}$ .

*Proof.* Consider a quadratic Lyapunov function  $V(x) = x^\top \text{P}x$ , with symmetric  $\text{P} > 0 \in \mathbb{R}^{n \times n}$ .

Note first that the satisfaction of inequality (11) means that matrix  $\bar{\text{X}}$  is non-singular. The satisfaction of relation (12) ensures the inclusion of the ellipsoid  $\varepsilon(\text{P}, 1)$  in the set given by  $\mathbb{S} = \{x \in \mathbb{R}^n; -\bar{u}_{(i)} \leq \text{G}_{(i)}x \leq \bar{u}_{(i)}\}$ , where  $\bar{\text{G}} = \text{G}\bar{\text{X}}^\top$ ,  $\text{P} = \text{X}\bar{\text{P}}\text{X}^\top$  and  $\text{X} = \bar{\text{X}}^{-1}$ .

Next we want to verify that  $\dot{V}(x) < 0$ . By choosing  $\theta = \text{C}x - \text{G}x$ , Lemma 1 applies and one gets  $-2\varphi^\top(y_f)\text{T}[\varphi(y_f) + \theta] \geq 0$ , for any  $x \in \mathbb{S}$ . Hence, if we verify that

$$\mathcal{L} = \dot{V}(x) - 2\varphi^\top(y_f)\text{T}[\varphi(y_f) + \theta] + e^\top \text{R}e < 0, \quad (13)$$

with  $\text{R} > 0$ ,  $\text{T} > 0$ , then  $\dot{V}(x) < 0$ , and stability of (8) is assured. Consequently,  $\dot{V}(x) + e^\top \text{R}e < 0$  is also satisfied, which can be integrated leading to

$$\int_0^\infty e(\tau)^\top \text{R}e(\tau) d\tau < V(x(0)) \leq 1, \quad (14)$$

which shows the bound on the energy of the signal  $e(t)$ . By defining the augmented vector  $\zeta = [\dot{x}^\top \quad x^\top \quad \varphi(y_f)^\top]^\top$ , we can rewrite inequality  $\mathcal{L} < 0$  as  $\mathcal{L} = \zeta^\top \text{Q}\zeta < 0$ , with

$$\text{Q} = \begin{bmatrix} 0 & \text{P} & 0 \\ \star & \text{H}^\top \text{R} \text{H} & \text{G}^\top \text{T}^\top - \text{C}^\top \text{T}^\top + \text{H}^\top \text{R} \text{M} \\ \star & \star & -2\text{T} + \text{M}^\top \text{R} \text{M} \end{bmatrix}. \quad (15)$$

We also have that the relation  $\bar{\text{B}}\zeta = 0$  holds for  $\bar{\text{B}} = [-\text{I} \quad \text{A} \quad \text{B}_\varphi]$ . From the Finsler Lemma, we have that the following facts are equivalent (see, for example, [2]):

- $\zeta^\top \text{Q}\zeta < 0$ ,  $\forall \zeta$  such that  $\bar{\text{B}}\zeta = 0$ ,  $\zeta \neq 0$ .
- $\exists \text{W}$  such that  $\text{Q} + \text{W}\bar{\text{B}} + \bar{\text{B}}^\top \text{W}^\top < 0$ .

By considering  $\text{W} = [\text{X}^\top \quad \text{X}^\top \quad 0]^\top$ , we obtain the new condition  $\Psi = \text{Q} + \text{W}\bar{\text{B}} + \bar{\text{B}}^\top \text{W}^\top < 0$ . By applying a Schur complement to  $\Psi$ , followed by pre- and post-multiplying by  $\text{diag}(\text{X}^{-1}, \text{X}^{-1}, \text{T}^{-1}, \text{I})$  and its transpose, respectively, and making changes of variable  $\bar{\text{R}} = \text{R}^{-1}$ ,  $\bar{\text{X}} = \text{X}^{-1}$ ,  $\bar{\text{P}} = \bar{\text{X}}\text{P}\bar{\text{X}}^\top$ ,  $\text{S} = \text{T}^{-1}$ ,  $\bar{\text{G}} = \text{G}\bar{\text{X}}^\top$ ,  $\text{K}_f = \text{A}_f \text{X}_{33}^\top$ ,  $\text{K}_e = \text{E}\text{S}$  we obtain condition  $\bar{\Psi} < 0$ . Hence, it follows that if relations (11) and (12) are satisfied then one gets  $\mathcal{L} < 0$ , or equivalently  $\dot{V}(x) < 0$ , for any  $x \in \varepsilon(\text{P}, 1)$ . Then the two items of Theorem 1 are proven and the proof is completed.  $\square$

**Remark 4.** In case the plant state matrix  $\text{A}_p$  is Hurwitz stable, global stability of the closed loop can be achieved and the design of  $\text{A}_f$ ,  $\text{E}_f$ ,  $\text{E}_c$  can also be realized by solving LMI (11) with  $\bar{\text{G}} = 0$ . Indeed, this case is straightforward by noticing that making  $\bar{\text{G}} = 0$  imposes that  $\text{G} = 0$  and therefore corresponds to making  $\theta = y_f$ , thus turning set  $\mathbb{S}$  into the whole state-space.

### 3.2 Case when M enters the plant

In some papers, as the one in [14], the influence matrix  $\text{M}$  enters the plant model. In this case,  $m_a = m_c$ , the system has more inputs than states ( $m_c > n_p$ ) and the input-redundancy nature of the plant is explicit. All the results in this paper can straightforwardly be applied in this case by making  $\text{M} = \text{I}$  and choosing  $\text{N}$  as a base for the null space of  $\text{B}_p$ , that is,  $\text{B}_p \text{N} = 0$ . Although in this case  $\text{M}\text{N} \neq 0$ , convergence of the allocator error to zero takes place due to the fact that the allocator states  $x_f$  converges to zero at steady-state, thus the term  $\text{N}x_f$  also tends to zero and the allocator recovers the property  $u_p = y_c$  after some time.

### 3.3 Optimization issues

From (14), it becomes clear that maximization of the trace of  $\mathbf{R}$  leads to minimization, in some sense, of the allocator error  $e(t)$ . Therefore, while solving the LMIs in Theorem 1 (or in Remark 4), we can accomplish better results for the allocator by minimizing the trace of  $\bar{\mathbf{R}}$ . In case of Theorem 1, the maximization of the ellipsoid  $\varepsilon(\mathbf{P}, 1)$  is also of interest. Therefore, a multi-objective convex optimization procedure applies. Consider a positive definite matrix  $\mathbf{P}_0$  and the following matrix inequality

$$\begin{bmatrix} \mathbf{P}_0 & \mathbf{I} \\ \star & \bar{\mathbf{X}} + \bar{\mathbf{X}}^\top - \bar{\mathbf{P}} \end{bmatrix} \geq 0. \quad (16)$$

Then, minimization of the trace of  $\mathbf{P}_0$  indirectly leads to minimization of the trace of  $\mathbf{P}$  and, therefore, to maximization of the ellipsoid  $\varepsilon(\mathbf{P}, 1)$ . Consider weighting parameters  $\rho_1, \rho_2$ . Then the following convex optimization procedure takes place in case of Theorem 1

$$\begin{aligned} & \min \rho_1 \lambda_1 + \rho_2 \lambda_2 \\ & \text{subject to (11), (12), (16), } \mathbf{P}_0 \leq \lambda_1 \mathbf{I}, \bar{\mathbf{R}} \leq \lambda_2 \mathbf{I} \end{aligned} \quad (17)$$

In case global asymptotic is sought (Remark 4), the following convex optimization procedure applies

$$\begin{aligned} & \min \lambda \\ & \text{subject to (11) with } \bar{\mathbf{G}} = 0 \text{ and } \bar{\mathbf{R}} \leq \lambda \end{aligned} \quad (18)$$

Since optimization problems (17) and (18) are convex, they can be easily solved with the help from standard LMI solvers and parsers (for example the YALMIP toolbox from [7]).

## 4 Simulation results

### 4.1 Example 1

Consider the satellite formation flying control problem from [1], where the controlled output  $y_p$  represents the relative position between two satellites in a vertical axis. Given two satellites, the objective is to cancel the lateral position error between them in the  $z$ -axis. The process can be represented by the following model

$$\left[ \begin{array}{c|c} \mathbf{A}_p & \mathbf{B}_p \\ \hline \mathbf{C}_p & \mathbf{D}_p \end{array} \right] = \left[ \begin{array}{cc|cc} 0 & 1 & 0 & 0 \\ 0 & 0 & m_1^{-1} & -m_2^{-1} \\ \hline 1 & 0 & 0 & 0 \end{array} \right],$$

where  $m_1^{-1}$  and  $m_2^{-1}$  are the masses of the two satellites. The plant input is given by  $u_p = [u_{p1}^\top \ u_{p2}^\top]^\top$ , where  $u_{p1}$  and  $u_{p2}$  are forces that act individually in each satellite. Each satellite possesses 4 thrusters that jointly produce the force applied in each of them. The influence matrix is given by  $\mathbf{M} = \text{diag}(\mathbf{M}_1, \mathbf{M}_2)$ , with  $\mathbf{M}_1 = \mathbf{M}_2 = \begin{bmatrix} 1 & -1 & -1 & 1 \end{bmatrix}$ . We assume that each thruster can produce a force between  $0$   $mN$  and  $100$   $mN$ , therefore the saturation limits are not symmetric. In order to apply the developed conditions, the same symmetrizing technique of [1] takes place, consisting of substituting the asymmetric saturation by a symmetric one with limits  $\bar{u}_i = 50$   $mN, i = 1 \dots 8$ , followed by addition of the kernel symmetrizing vector  $\xi = \bar{u}$ . After choosing  $m_1 = m_2 = 1000$   $kg$ , a stabilizing LQG controller is designed using identity matrices for all the weights. The resulting controller is given by

$$\left[ \begin{array}{c|c} \mathbf{A}_c & \mathbf{B}_c \\ \hline \mathbf{C}_c & \mathbf{D}_c \end{array} \right] = \left[ \begin{array}{cc|c} -1.7321 & 1 & 1.7321 \\ -1.0014 & -0.0532 & 1 \\ \hline -0.7071 & -26.6009 & 0 \\ 0.7071 & 26.6009 & 0 \end{array} \right],$$

We then compute  $M^\dagger = 0.25 \text{diag}(M_1^\top, M_2^\top)$ ,  $N = \text{diag}(N_1, N_2)$ , with  $N_1 = N_2 = \begin{bmatrix} 1 & 1 & -1 \\ & & I_3 \end{bmatrix}$ . We use optimization procedure (17) with weights  $\rho_1 = 1, \rho_2 = 0.15$ , so that regional asymptotic stability can be guaranteed by means of Theorem 1. The obtained anti-windup and allocator matrices for this example are given by

$$\begin{bmatrix} E_c \\ E_f \end{bmatrix} = \begin{bmatrix} -0.0360 & -0.0380 & 0.0978 & -0.0979 & 0.0918 & -0.0921 & -0.0921 & 0.0921 \\ -0.0379 & 0.0057 & 0.0664 & -0.0664 & 0.0636 & -0.0639 & -0.0639 & 0.0639 \\ 0.0991 & 0.0676 & -0.0051 & -0.0037 & -0.0050 & -0.0127 & -0.0126 & 0.0127 \\ -0.0991 & -0.0676 & -0.0037 & 0.0983 & 0.1000 & 0.0100 & 0.0099 & -0.0099 \\ 0.0929 & 0.0647 & -0.0050 & 0.0999 & 0.0859 & -0.0158 & -0.0158 & 0.0158 \\ -0.0933 & -0.0649 & -0.0127 & 0.0100 & -0.0158 & 0.2498 & -0.1298 & 0.1298 \\ -0.0933 & -0.0649 & -0.0126 & 0.0099 & -0.0158 & -0.1298 & 0.2498 & 0.1298 \\ 0.0933 & 0.0649 & 0.0127 & -0.0099 & 0.0158 & 0.1298 & 0.1298 & 0.2498 \end{bmatrix},$$

$$A_f = \begin{bmatrix} -1.7554 & -2.3389 & 2.3338 & -0.0027 & -0.0027 & 0.0027 \\ -0.3432 & -2.9489 & 0.1056 & 0.0452 & 0.0452 & -0.0452 \\ 0.4526 & -0.0022 & -2.8405 & 0.0488 & 0.0488 & -0.0488 \\ -0.6866 & 0.7027 & -0.7039 & -2.7942 & -0.0915 & 0.0915 \\ -0.6866 & 0.7027 & -0.7039 & -0.0916 & -2.7943 & 0.0916 \\ 0.6866 & -0.7027 & 0.7039 & 0.0916 & 0.0916 & -2.7942 \end{bmatrix}.$$

We simulate the system response for an initial condition of  $x_p(0) = [-0.25 \quad 0.001]^\top$ , with  $x_c(0) = 0$  and  $x_f(0) = 0$ . Figure 3 shows the obtained results. It can be observed that the allocation error is indeed reduced by application of the proposed technique.

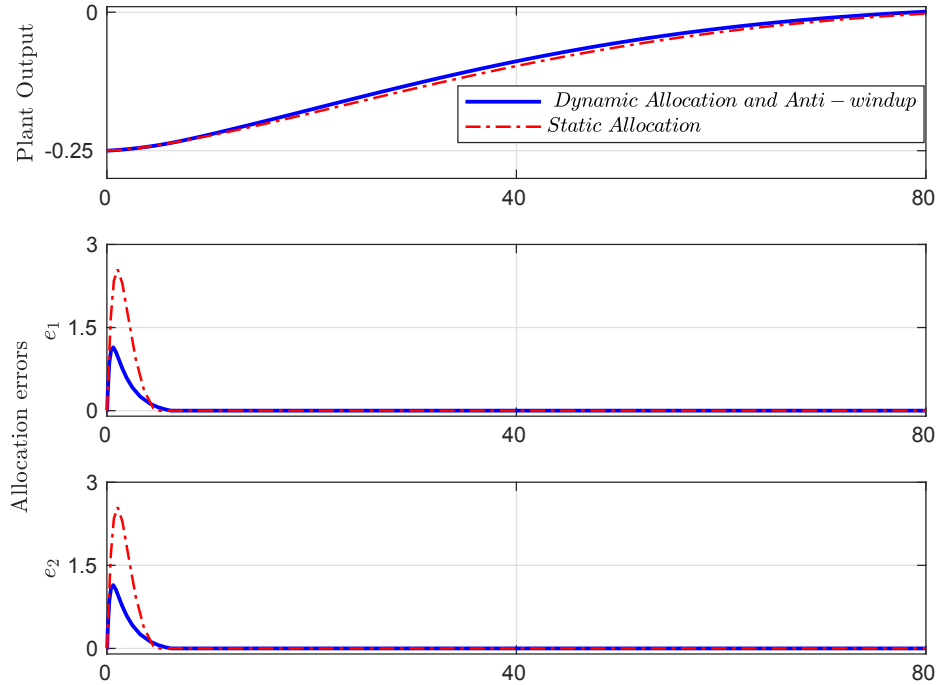


Figure 3: Example 1: Output and allocation errors.

## 4.2 Example 2

Consider the exponentially stable plant from [14]. The plant is defined by the following data:

$$\left[ \begin{array}{c|ccc} \mathbf{A}_p & \mathbf{B}_p & & \\ \hline \mathbf{C}_p & \mathbf{D}_p & & \end{array} \right] = \left[ \begin{array}{cc|cc} -0.157 & -0.094 & 0.87 & 0.253 & 0.743 \\ -0.416 & -0.45 & 0.39 & 0.354 & 0.65 \\ \hline 0 & 1 & 0 & 0 & 0 \end{array} \right].$$

There is no loss of generality in considering this example since  $\mathbf{D}_p = 0$ . This process is input redundant, as noted in [14]. The saturation limits are given by  $\bar{u} = [1 \ 0.01 \ 0.02]^\top$ . To control the system and guarantee asymptotic tracking of constant references in the absence of saturation, [14] inserts an integrator and designs a stabilizing LQG controller which only uses the first two input channels. The resulting controller is given by

$$\left[ \begin{array}{c|ccc} \mathbf{A}_c & \mathbf{B}_c & & \\ \hline \mathbf{C}_c & \mathbf{D}_c & & \end{array} \right] = \left[ \begin{array}{cccc|c} -1.57 & 0.5767 & 0.822 & -0.65 & 0 \\ -0.9 & -0.501 & -0.94 & 0.802 & 0 \\ 0 & 1 & -1.61 & 1.614 & 0 \\ 0 & 0 & 0 & 0 & -1 \\ \hline 1.81 & -1.2 & -0.46 & 0 & 0 \\ -0.62 & 1.47 & 0.89 & 0 & 0 \\ 0 & 0 & 0 & 0 & 0 \end{array} \right].$$

For this example,  $m_a = m_c$  and  $\mathbf{M} = \mathbf{I}$ . We select then  $\mathbf{N}$  as the Kernel of  $\mathbf{B}_p$ , resulting in  $\mathbf{N} = [-0.4726 \ -1.3143 \ 1]^\top$ . In this case, we utilize optimization procedure (18) which allows to establish global asymptotic stability results (Remark 4). We obtain, thus

$$\left[ \begin{array}{c} \mathbf{E}_c \\ \mathbf{E}_f \end{array} \right] = \left[ \begin{array}{ccc} 0.0805 & 0.1071 & -0.5001 \\ 0.6952 & -0.3965 & -0.4768 \\ -5.1823 & 2.5204 & -0.3478 \\ -4.0392 & 2.7077 & -0.0247 \\ \hline -1.3366 & -0.2536 & 0.1016 \end{array} \right], A_f = -72.8135.$$

The parameters of the allocator and the anti-windup of [14] can be found therein. Since we are dealing with the stabilization case, we consider null reference and simulate the system response for an initial condition  $x_p(0) = [0.4 \ 0.4]^\top$ , with  $x_c(0) = 0$  and  $x_f(0) = 0$ . Figure 4 shows the output response and the allocator errors for both strategies. The computed control signal and the plant input for the proposed strategy and the one from [14] are shown in Figures 5 and 6, respectively. The fundamental difference in the results relies in the fact that for the proposed strategy, the allocator error is kept very small during the whole simulation and converges to zero after the system is out of saturation. It should be reminded, however, that minimizing the allocator error was not a priority in [14].

## 5 Conclusion

In this paper, we proposed the co-design of dynamic allocation function and anti-windup loop in the presence of saturation of actuators. The allocation function has a general format, which allows to include multiple objective criteria into the design conditions. The developed equations can be used in both the cases when the controller is designed by taking into account the process model from forces and torques and the case when the process model explicitly exhibits the over-actuation phenomenon, that is, when the influence matrix  $\mathbf{M}$  enters the process model. Simulation case studies were used to illustrate both cases. The results open the door for several future work as in particular to consider other nonlinearities affecting the actuator and the fact to deal with event-triggered control.

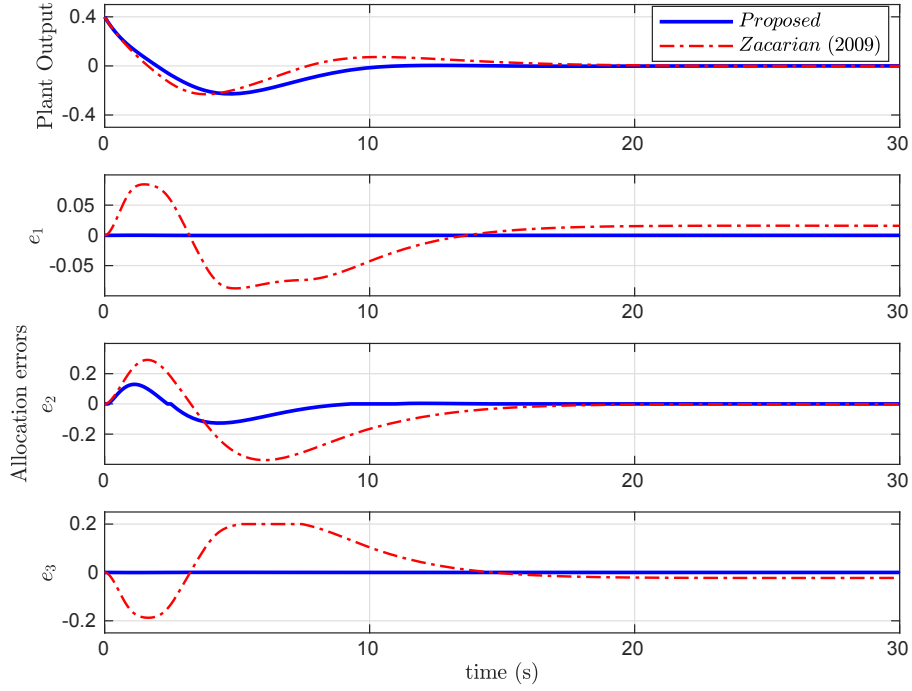


Figure 4: Example 2: Output and allocation errors for both the proposed strategy and [14].

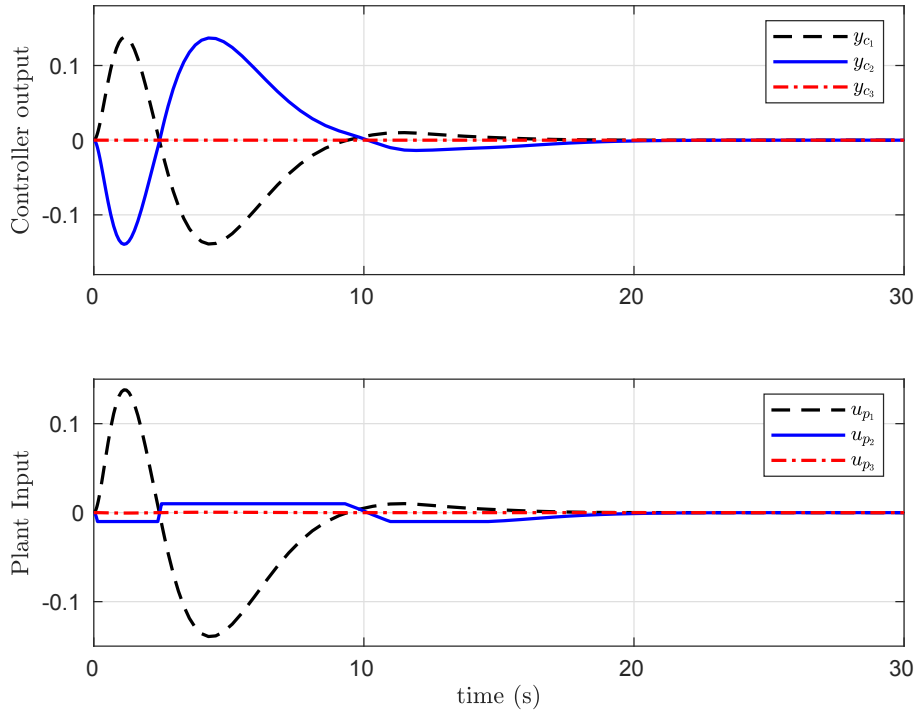


Figure 5: Example 2: Controller output and plant input signals for the proposed strategy.

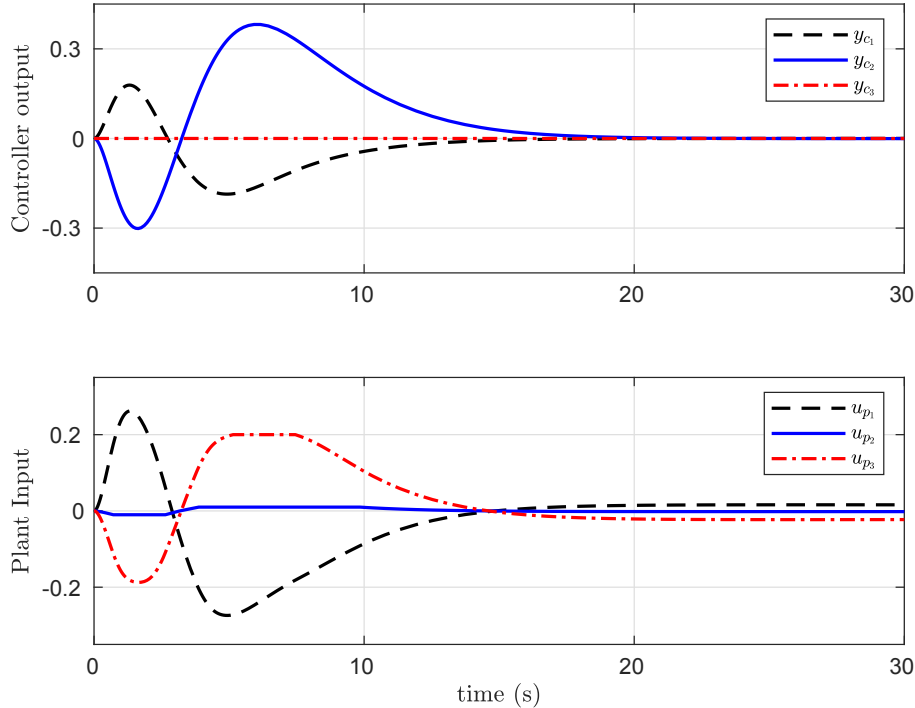


Figure 6: Example 2: Controller output and plant input signals for the strategy from [14].

## Acknowledgment

This study was financed in part by the Coordenação de Aperfeiçoamento de Pessoal de Nível Superior - Brasil (Capes) - Finance Code 001, and by ANR project HANDY 18-CE40-0010.

## References

- [1] Josep Boada, Christophe Prieur, Sophie Tarbouriech, Christelle Pittet, and Catherine Charbonnel. Formation flying control for satellites: Anti-windup based approach. In Giorgio Fasano and János D. Pintér, editors, *Modeling and Optimization in Space Engineering*, pages 61–83. Springer New York, New York, NY, 2013.
- [2] Maurício C. de Oliveira and Robert E. Skelton. Stability tests for constrained linear systems. In S.O. Reza Moheimani, editor, *Perspectives in robust control*, pages 241–257, London, 2001. Springer London.
- [3] Wayne Durham, Kenneth A. Bordignon, and Roger Beck. *Aircraft Control Allocation*. John Wiley & Sons, Ltd, December 2016.
- [4] Sergio Galeani, Andrea Serrani, Gianluca Varano, and Luca Zaccarian. On input allocation-based regulation for linear over-actuated systems. *Automatica*, 52:346 – 354, 2015.
- [5] Jaehyun Jin. Modified pseudoinverse redistribution methods for redundant controls allocation. *Journal of Guidance, Control, and Dynamics*, 28(5):1076–1079, September 2005.
- [6] Tor A. Johansen and Thor I. Fossen. Control allocation—a survey. *Automatica*, 49(5):1087 – 1103, 2013.
- [7] J. Löfberg. Yalmip : A toolbox for modeling and optimization in matlab. In *In Proceedings of the CACSD Conference*, Taipei, Taiwan, 2004.

- [8] M. W. Oppenheimer, D. B. Doman, and M. A. Bolender. Control allocation for over-actuated systems. In *2006 14th Mediterranean Conference on Control and Automation*, pages 1–6, June 2006.
- [9] J. A. M. Petersen and M. Bodson. Constrained quadratic programming techniques for control allocation. *IEEE Transactions on Control Systems Technology*, 14(1):91–98, Jan 2006.
- [10] A. Serrani. Output regulation for over-actuated linear systems via inverse model allocation. In *2012 IEEE 51st IEEE Conference on Decision and Control (CDC)*, pages 4871–4876, Dec 2012.
- [11] E. D. Sontag. An algebraic approach to bounded controllability of linear systems. *Int. J. Control*, 39(1):181–188, 1984.
- [12] S. Tarbouriech, G. García, J. M. Gomes da Silva Jr., and I. Queinnec. *Stability and Stabilization of Linear Systems with Saturating Actuators*. Springer, London, 2011.
- [13] Johannes Tjønnås and Tor A. Johansen. Adaptive control allocation. *Automatica*, 44(11):2754 – 2765, 2008.
- [14] Luca Zaccarian. Dynamic allocation for input redundant control systems. *Automatica*, 45(6):1431 – 1438, 2009.
- [15] Luca Zaccarian and Andrew R. Teel. *Modern Anti-windup Synthesis: Control Augmentation for Actuator Saturation (Princeton Series in Applied Mathematics)*. Princeton University Press, 2011.